

Electrical contact resistance and wear of a dynamically excited metal–graphite brush

Aleš Turel¹, Janko Slavič² and Miha Boltežar²

Abstract

The wear and contact resistance of sliding contacts are typically researched with a pin-on-disk experiment that prevents dynamic excitation. However, in electrical machines, the brush clearance enables dynamic excitation, resulting in flexible body dynamics. To research the wear and contact resistance during dynamical excitation, an in-situ experimental approach is introduced here, with the influences of rotational speed, electrical current, and temperature being assessed. This research shows that a small wear rate and contact resistance are possible at 10,000 and 5000 RPM if the electrical current is higher than 3 A. It was also found that the contact resistance decreased with an increased ambient temperature, electrical current, and rotating speed, whereas the wear rate increased with the rotating speed at low current density and low ambient temperature.

Keywords

Sliding contact, metal-matrix composite, electric contacts, wear rate, contact resistance

Date received: 16 June 2016; accepted: 27 January 2017

Academic Editor: Mario L Ferrari

Introduction

Electrical machines have been in service for decades; however, their mass and energy density are still being optimized and the electrical brushes significantly affect the life times of these electrical machines. The goal to decrease the uncertainty of the brush's lifetime is therefore a high priority.¹ The lifetime of alternators is dependent on the electro-mechanical contact between the slip-ring and the brush,² while the electro-mechanical contact depends on the brush dynamics, for example, on the rotational speed of the slip-ring, the vibrations, the spring force, the coefficient of friction, the ambient parameters, the wear, and the electrical current.²

In the past, electrical brushes have been widely researched: Hu et al.³ found that for an electrographite brush running against a copper commutator, the oxide film thickness increases (which increases the electrical resistance and consequently the wear of the brushes) if

the current density is increased. Furthermore, the air humidity influences the formation of the oxide film: Hu et al. found that at 10%rH humidity, the wear rate of a fixed brush was about two times higher than at 50%rH humidity (for the same current density).

The wear mechanisms of an electrical sliding contact between graphite and copper were studied by Senouci et al.,⁴ who found that the wear behavior can be correlated with the surface morphology of the graphite orientation in the contact (the hardness of the graphite surface). Furthermore, Senouci et al. observed

¹MAHLE Letrika d.o.o., Šempeter pri Gorici, Slovenia

²Faculty of Mechanical Engineering, University of Ljubljana, Ljubljana, Slovenia

Corresponding author:

Miha Boltežar, Faculty of Mechanical Engineering, University of Ljubljana, Aškerčeva 6, 1000 Ljubljana, Slovenia.

Email: miha.boltezar@fs.uni-lj.si



a decrease in the coefficient of friction and a difference in the wear between the anode and the cathode brushes. The irregular wear of fixed brushes was also researched by Argibay et al.⁵ They observed differences between the brushes in terms of the coefficient of friction, the contact resistance, and the temperature. Abrupt changes in the temperature, the contact resistance, and the friction were found by Jensen⁶ when he researched the wear of high-current-density electrical brushes. Jensen found that the changes in the wear rate are slow (within a few hours). The wear rate of a carbon-graphite material was also studied by Zhao et al.,⁷ who researched the coefficient of friction and wear in terms of the electrical current, a high sliding speed, and a normal load. Zhao et al.⁷ found that the wear rate follows Archard's law when the contact was without any electrical current.

The influences of brush wear and brush stiffness were studied by Slavič et al.⁸ They researched the dynamic stability of an electrical motor's brush using numerical simulations. Slavič and Boltežar⁹ also researched a wear model on the local loss of mechanical energy under dynamical loads, the brush dynamics with a rough contact surface,¹⁰ and identified the coefficient of friction for different temperatures and currents.^{11,12} The measurements were made on a fixed brush. Slavič et al.¹³ also researched the influence of surface roughness, where they found that a random roughness leads to distinct vibrations that increase with wear. Surface roughness was also researched by Ueno et al.¹⁴ They were focused on the surface roughness and the voltage drop and found that the contact-voltage drop changed with different surface-roughness conditions in a vacuum.¹⁵ Furthermore, Ueno and Morita¹⁶ observed that the contact-voltage drop increases with a decrease in the real contact area.

Zhongliang et al.¹⁷ studied the influence of the contact pressure and the rotational speed on the wear of carbon brushes. They found that the wear of the brushes depends on the pressure-velocity (PV) factor (the product of the contact pressure and the peripheral speed). If the PV factor was below the critical value, the contact film was good and dominated the mechanical wear. If the PV factor was above the critical value, then the electrical wear is dominant (increasing exponentially).¹⁷ Similar research on copper-graphite brushes was presented by Yasar et al.¹⁸ They studied the effect of the brush-spring pressure on the wear behavior of the brushes at a constant rotating speed, electrical current, and ambient temperature using a pin-on-slip-ring test, where they observed the minimal wear of a copper-graphite brush at 30–50 kPa brush-spring pressure.

Recently, the contact resistance of a sliding contact was researched by Barnawi et al.¹⁹ They found an increase in the wear rate when the atmospheric

temperature decreases. Furthermore, they confirmed that the contact-voltage drop is lower at higher ambient temperatures. The effect of the electrical current was researched by Wang et al.²⁰ They observed that the wear loss increased with an increase in the electrical current and also a lower friction coefficient with an applied electrical load. The effect of sliding velocity on the transition of the wear mechanism was studied by Wang et al.²¹ They found that with an increase in the sliding velocity, the wear initially decreases and then increases. Fakihi and Dienwiebel²² found the formation of a thick layer on the commutator and on the brush surface as the main reason for the motor's failure. The effects of the contact pressure and the sliding velocity on the relationship between the electrical and mechanical wear of the brushes were studied by Wang et al.²³

This introduction shows that the contact resistance, the temperature, the electrical current, and the wear rate are usually researched with a fixed brush or using a pin-on-disc/slip-ring, where the dynamical motion of the brush is prevented. In the application, the brush can typically move with respect to the brush-holder clearance and the tension spring; this research assumes that the dynamics of the brush significantly influences the electrical contact resistance and the wear rate.

Brush material and its properties

Metal-graphite brush as a metal-matrix composite (MMC) specimen was manufactured by the powder metallurgy technique.²⁴ The manufacturing process was divided into four steps: raw material processing, mixing, shaping, and baking. In the first step, the raw materials of copper and graphite were grounded. Then, copper, graphite, and additives were mixed. The mixed powders were then cold pressed to fabricate a brush with dimensions of 6.4 mm × 4.6 mm and 16.5 mm length. The green specimen was finally sintered.

To characterize particles in the MMC, the microstructural studies were carried out. Metal-graphite brush was prepared, and then scanning electron microscopic (SEM) image was taken. SEM image of metal-graphite brush is presented in Figure 1. The black areas are graphite particles—approximately 60 wt%. The graphite particles are uniformly distributed through the MMC. The space between graphite is full filled by copper and additives (light areas)—approximately 40 wt%.

The average values of mechanical properties such as density and hardness of metal-graphite brush were 2.5 g/cm³ and 19.0 HsD respectively.

Experimental setup

To research the key parameters affecting the wear of the brushes, the test setup shown in Figure 2 was used.

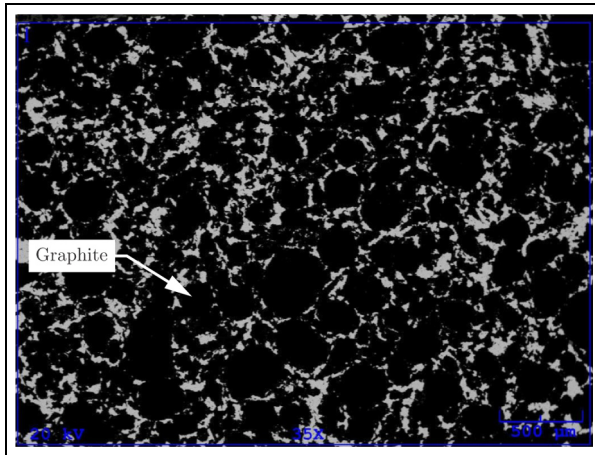


Figure 1. Microstructure of metal-graphite brush.

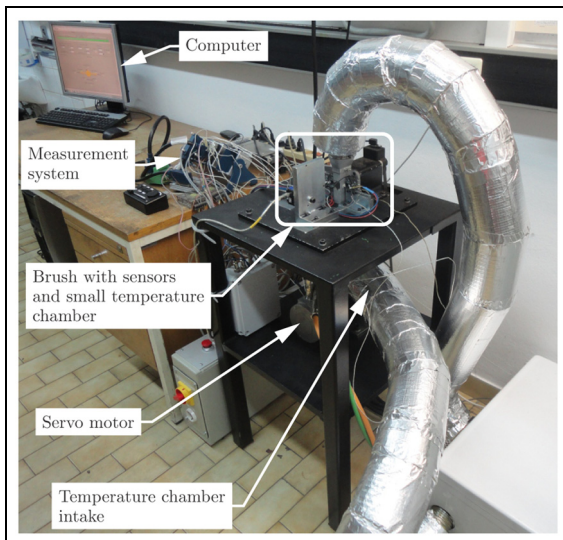


Figure 2. Test setup.

The drive part of the setup consists of a 2.5-kW, three-phase servo motor, tensioner, and vibroinsulation. Figure 3 shows the measuring part of the setup, and it consists of a rigid bearing housing, a drive shaft, two brush holders, and a small temperature chamber. The drive shaft is driven with a belt to simulate real conditions. On the opposite end of the shaft, small copper slip-rings with a diameter of 16.4 mm are used. The maximum sliding speed at the slip-ring peripheral is 15 m/s. One pair of brushes can be tested at a time. The electrical current of 0–5 A was delivered to the brush via a standard flexible wire (as used in serial production; see Figure 3). Figures 2 and 3 show the slip-rings and brushes enclosed in a small temperature chamber equipped with K-type thermocouples, which simulates the conditions in an application. The testing conditions are shown in Table 1 and will be discussed in detail later.

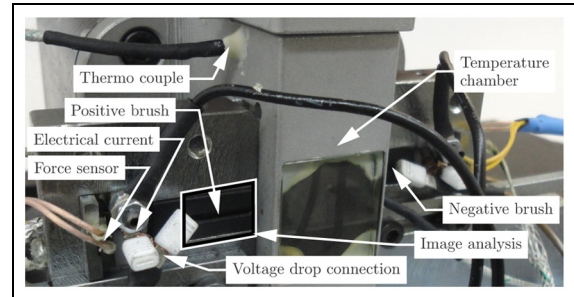


Figure 3. Brush close-up.

Table 1. Test operating parameters and conditions.

Parameter	Value
Number of brushes	Two brushes (positive and negative)
Brush nominal surface area	29.44 mm ² (6.4 mm × 4.6 mm)
Brush material	Metal-graphite (40 wt% Cu, 60 wt% C)
Brush normal force	2.4 N
Slip-ring nominal diameter	16.4 mm
Slip-ring material	Copper (SE-Cu F25)
Slip-ring rotational speed	1000, 5000, and 10,000 RPM
Electrical current (DC)	1, 2, 3, 4, and 5 A
Atmosphere	Ambient air
Ambient temperature	22°C, 40°C, and 80°C
Ambient humidity	40–60%rH
Test duration	15–100 h

Drive motor and rotational speed

The drive motor for rotating the shaft with slip-rings is a three-phase brushless servo motor (Unimotor FM 115U2; Emerson Industrial Automation) with a nominal speed of 6000 RPM and 6.6 Nm of nominal torque. The motor is connected and controlled with a servo regulator (Unidrive SP 1406; Emerson Industrial Automation). The servo regulator is controlled by an analog input port connected with an NI 9269 (analog output card) on an NI cDAQ-9178 and software. Because the shaft was driven by a pulley, the rotational speed of the shaft was measured using an encoder and a Hall-effect speed sensor.

Brush holder and sensors

A small gap for image analysis was added to the serially produced brush holder (see Figure 3). The contact force was applied using a helical spring that was placed between the force sensor and the brush (see Figure 4). The axial force on the spring was measured with a microelectromechanical system (MEMS) force sensor (FSS1500NSB; Honeywell). The temperature of the force sensors (used for temperature corrections) and

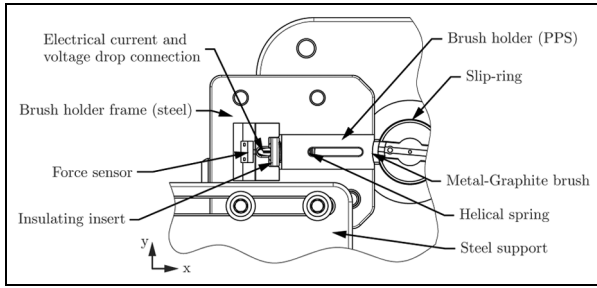


Figure 4. Instrumented brush holder without temperature chamber.

the brush holder were measured with a K-type thermal probe.

A 0.2-mm clearance between the brush and the brush holder was used. As the researched brush's mass was 1.5 g (including the flexible wire), the brush dynamics would be significantly influenced by a contact-displacement sensor or if the brush was fixed. Therefore, the brush wear was estimated via digital image correlation (DIC) using displacement measurements (mvBlueFOX; Matrix Vision). The DIC approach was verified by manual measurements before and after the test.

Climate-conditions control and measurement

The temperature chamber equipped with K-type thermocouples is shown in Figure 3. On the top and bottom sides of this small chamber were two openings that were connected with a larger 26-L volume temperature chamber in which a 2.1-kW heater was placed. With the heater, an air blower, and an additional heat gun mounted on the slip-ring compartment, air-temperatures from 22°C to 200°C with a tolerance of $\pm 2^\circ\text{C}$ were achieved. Additionally, the humidity of the air was measured³ (177-H1; TESTO) (see Table 1).

Power supply with current and voltage-drop measurements

A power supply (HWS600-2; TDK Lambda) connected with a metal-oxide-semiconductor field-effect transistor (MOSFET, BDX53C; ST) delivered 0- to 5-A DC current to the brush-slip-ring contact. Wires were attached to the end of brushes' flexible wire (see Figure 4). The power supply with a MOSFET, which was controlled by a NI analog output (NI 9269), maintains the current with an accuracy of ± 0.01 A.

The electrical current was measured using a Hall sensor (LA 50-S; LEM) at the positive brush wire, while the voltage drop (NI 9239) was measured for both brushes (see Figure 5).

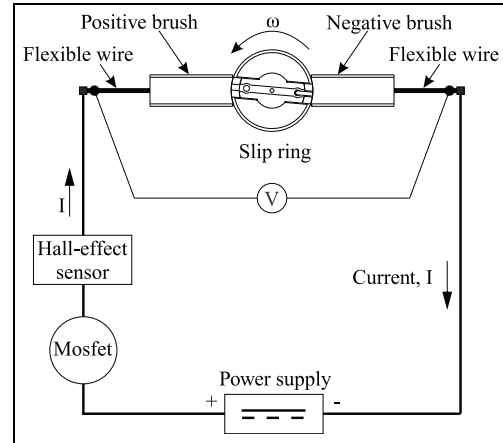


Figure 5. Electrical circuit diagram of the test bench.

Control and data-logging

The control and data-logging software for the test bench was developed in LabView 2013. A National Instruments cDAQ-9178 chassis with six different modules was used to acquire the signals. Each minute, a 60-s measurement, sampled at 5000 S/s, was averaged and saved (one averaged record per minute).

Test conditions and running-in

Each test started with a new set of slip-rings (with a shaft) and brushes. Before the test, the slip-rings' surface parameters (roundness and roughness) were measured. After the test setup, a running-in period of 100 h at ambient temperature was started to establish steady running-in contact conditions. The test duration was typically 15–100 h. Details about the test conditions are given in Table 1.

Brush contact-resistance identification

The brush contact resistance, which represents the electrical contact situation between the positive and negative brushes, is defined as

$$R_{\text{contact}} = \frac{V_{\text{contact}}}{I_{\text{contact}}} \quad (1)$$

where V_{contact} is the contact-voltage drop and I_{contact} is the electrical current. An increase in the contact resistance is connected with a decrease in the real contact area.¹⁶

Brush wear-rate optical identification

The position of the brush, defined by the center point and the area of the brush next to the helical spring, is tracked via the DIC. The initial position at the start of

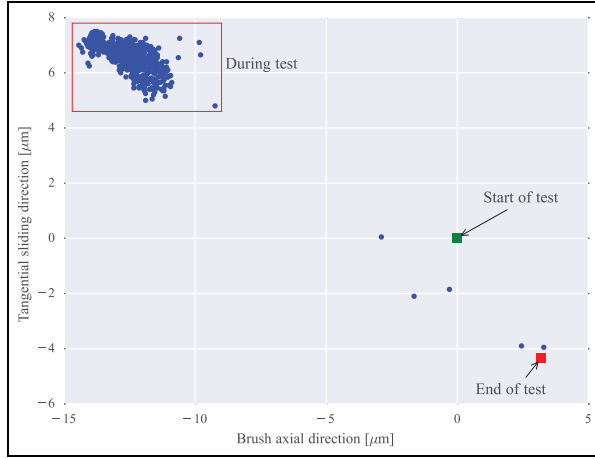


Figure 6. Position of the brush in axial and tangential directions (1000 RPM at 22°C for 15 h).

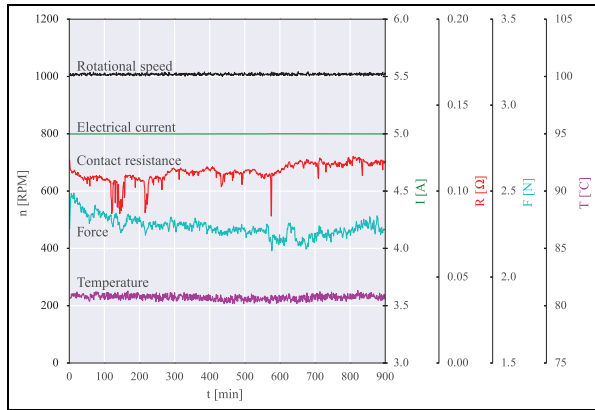


Figure 7. Rotational speed, electrical current, temperature in the slip-ring compartment, contact resistance, and normal force during the test.

the test is measured at rest when the slip-ring is not rotating (see Figure 6). During the test, the brush changes its position primarily as a result of the dynamic response with regard to the contact with the slip-ring. At the end of the test (at rest), the final position is identified again. From the difference between the final position s_2 and the initial position s_1 , the wear rate w is identified as

$$w = \frac{s_2 - s_1}{t \cdot v} \quad (2)$$

where t is the test duration and v is the tangential rotational speed.

Measurement

As an example, Figure 7 shows the test results at 1000 RPM, 5-A electrical current, and 80°C ambient temperature in the slip-ring compartment. The

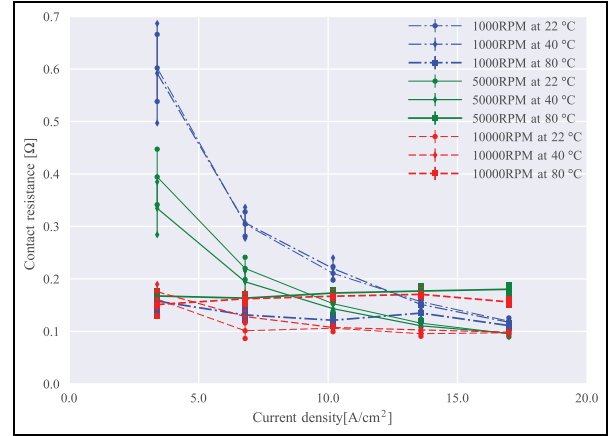


Figure 8. Contact resistance versus electrical current density, rotational speed, and temperature.

temperature in the slip-ring compartment was stabilized at the beginning of the test. Because the contact situations during the test were changing,⁶ the temperature in the compartment was also changing (see Figure 7). Figure 7 shows how the contact resistance and the normal contact force were changing for a constant rotational speed and electrical current. The contact resistance increased by 0.9 mΩ during the test. A maximum of 0.12 Ω was observed after 809 min and a minimum of 0.08 Ω at 576 min. At 577 min, a minimum normal contact force of 2.16 N was observed; the maximum 2.48 N force was observed 5 min after the beginning of the test. The normal contact force decreased by 0.005 N during the test. Similar results as shown in Figure 7 were obtained under different operating conditions (Table 1); however, in the next section, only the averaged results will be discussed.

Results

As shown in Table 1, the influences of the slip-ring's rotational speed (1000, 5000, and 10,000 RPM), the electrical current (1, 2, 3, 4, and 5 A), and the ambient temperature (22°C, 40°C, and 80°C) were tested against the contact resistance and the wear rate. The number of different testing conditions is $3 \times 5 \times 3 = 45$, resulting in a total testing time of approximately 5400 h \approx 225 days. The results discussed below represent the average values of the two brushes (tested under a particular set of test conditions). The presented wear-rate results are for the positive brush only.

Contact resistance versus electrical current, rotational speed, and temperature

The contact resistance in relation to the electrical current density, the rotational speed, and the temperature is shown in Figure 8.

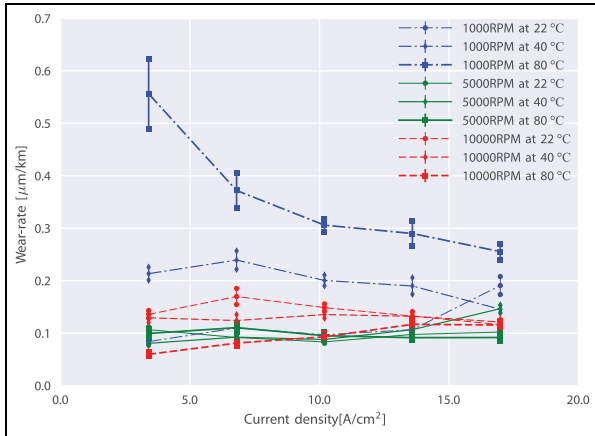


Figure 9. Wear rate versus electrical current density, rotational speed, and temperature.

In general, the contact resistance should be as small as possible. It decreases with an increase in the real contact area,¹⁶ and it is widely recognized that the real contact area can increase with the applied load. Nevertheless, the results in Figure 8, which at a constant applied load, show that with an increased electrical current density, temperature, and rotating speed, the contact resistance decreases for all the tests, except for the tests at 80°C and 5000 or 10,000 RPM. The decrease in the contact resistance can also connect with an increase in the electrical conduction area,²⁵ and a decrease in the brush stiffness with an increase in the temperature.¹² At the same time, additional open circuits become closed circuits and increase the real contact area. The hypothesis is that the contact resistance should be as small as possible due to the better contact situations.

Wear rate versus the electric current, rotating speed, and temperature

The wear rate in relation to the electrical current density, the rotational speed, and the temperature is shown in Figure 9. The wear rate should be as small as possible to find the optimum operating conditions.

The conclusions from the wear-rate results are not as straightforward as with the contact resistance. At 1000 RPM, the wear rate increases with the ambient temperature. At 5000 RPM, the temperature does not have a significant influence. At 10,000 RPM, the wear rate is the smallest at 80°C and 1-A and it increases with the electrical current; so that at 22°C and 40°C, the electrical current does not significantly influence the wear rate. To ensure the repeatability of the results, each test was repeated at least once.

The hypothesis is that the contact situations are optimal due to the small contact resistance and the small wear rate. To obtain a better insight into the contact

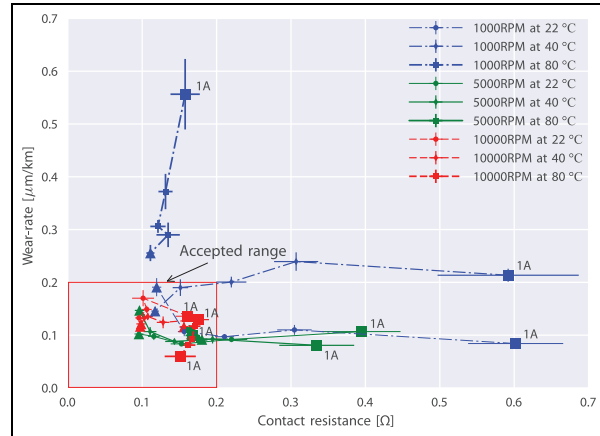


Figure 10. Wear rate versus contact resistance, electrical current, rotational speed, and temperature.

resistance and the wear-rate dependency, Figure 10 is used. Figure 10 shows the results already shown in Figures 8 and 9: the 1-A electrical current test is marked with square and the 5-A with a triangle.

Figure 10 shows that a small wear rate and contact resistance is possible at 10,000 and at 5000 RPM if the electrical current is higher than approximately 3-A. Finally, at 1000 RPM, good wear and contact conditions are possible for a high electrical current and low ambient temperature.

According to all the tests, the brush temperature is the main common point. From additional temperature measurements of the brush with infrared (IR) temperature camera, we observed that if the brush temperature was higher than 60°C, the contact resistance and the wear rate were in optimal range. From these results, we can conclude that minimal brush temperature is needed for good contact conditions, which can relate with Slavič and Boltežar's¹² findings where they found that the brush stiffness decreases with an increasing temperature up to 240°C.

To view the wear mechanism of the brush, the images of the worn brush contact surface with magnification 200× were taken. The appearance of the worn brush contact surface as shown in Figure 11 indicates the abrasive wear. The abrasive grooves are parallel to the sliding direction as a consequence of abrasive action by hard asperities or particles. Harder asperities are part of slip-ring where hardness is 105 HB, while the harder particles are wear parts of the brush, especially graphite. Irrespective of test conditions, we observed the domination of abrasive wear mechanism.

Discussion

For similar pairing materials, Wang et al.²⁰ found that the wear rate increases with an increase in the electrical current density (at a constant ambient temperature and

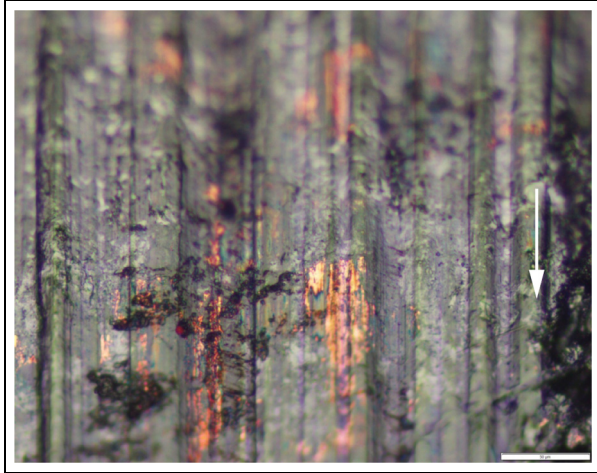


Figure 11. Brush worn contact surface.

rotational speed). Wang et al.'s findings are similar to our own; however, here, it has been additionally found that at high temperatures and/or high rotational speeds, the wear rate increases with the current density.

For copper-impregnated, metalized carbon, a brush sliding against a Cu–Cr–Zn slip-ring Wang et al.²³ observed an increase in the wear rate with an increase in the contact pressure. A similar finding was made by Zhao et al.⁷ for a carbon–graphite brush sliding against steel (tested with a pin-on-slip ring). Here, it has been found that at a constant contact pressure, the wear rate increases, however, only if the current density and ambient temperature are low.

Yasar et al.¹⁸ researched a different material pair (copper–graphite brush sliding against a steel slip-ring) and varied the brush-spring pressure; however, for the brush-spring force, they found that the friction initially decreases and finally increases. Yasar et al.'s report is relevant to this research as it shows that optimal operating conditions can significantly reduce the wear rate (and the contact resistance).

Conclusion

This research introduces an in-situ approach to researching the contact resistance and the wear rate of a brush sliding against a slip-ring, including the dynamical phenomena. The contact resistance and wear rate were researched using a controlled electrical current, rotating speed, and environmental temperature.

Tests at rotating speeds of 1000, 5000, and 10,000 RPM, electrical currents of 1, 2, 3, 4, and 5 A, and ambient temperatures of 22°C, 40°C, and 80°C were conducted. The results are based on 45 tests (repeated twice, total 90 tests) where new slip-rings and brush pairs were tested: after the running-in period of approximately 100 h, a test run for an additional 20 h

was usually performed. The contact resistance was found to decrease with an increased ambient temperature, electrical current, and rotating speed, while the wear rate was found to increase with the rotating speed at a low current density and a low ambient temperature. When at a high ambient temperature and a low current density, the wear rate decreases with an increase in the rotating speed. Consequently, it can be concluded that for the dynamically excited brush and the optimum rotational speed, an electrical load and ambient temperature are needed for a small contact resistance and wear rate.

Declaration of conflicting interests

The author(s) declared no potential conflicts of interest with respect to the research, authorship, and/or publication of this article.

Funding

The author(s) received no financial support for the research, authorship, and/or publication of this article.

References

1. Duffy O and Wright G. *Fundamentals of medium/heavy duty commercial vehicle systems* (Jones & Bartlett learning Cdx automotive). Burlington, MA: Jones & Bartlett Learning, 2015.
2. Slade P. *Electrical contacts: principles and applications* (electrical and computer engineering). Abingdon: Taylor & Francis, 1999.
3. Hu Z, Chen Z and Xia J. Study on surface film in the wear of electrographite brushes against copper commutators for variable current and humidity. *Wear* 2008; 264: 11–17.
4. Senouci A, Frene J and Zaidi H. Wear mechanism in graphite–copper electrical sliding contact. *Wear* 1999; 225–229: 949–953.
5. Argibay N, Bares J and Sawyer W. Asymmetric wear behavior of self-mated copper fiber brush and slip-ring sliding electrical contacts in a humid carbon dioxide environment. *Wear* 2010; 268: 455–463.
6. Jensen M. Long-term high resolution wear studies of high current density electrical brushes. In: *Proceedings of the fifty-first IEEE Holm conference on electrical contacts*, Chicago, IL, 26–28 September 2005, pp.304–311. New York: IEEE.
7. Zhao H, Barber G and Liu J. Friction and wear in high speed sliding with and without electrical current. *Wear* 2001; 249: 409–414.
8. Slavič J, Nastran M and Boltežar M. Modeling and analyzing the dynamics of an electric-motor brush. *J Mech Eng* 52: 2006; 126–137.
9. Slavič J and Boltežar M. Simulating multibody dynamics with rough contact surfaces and run-in wear. *Nonlinear Dynam* 2006; 45: 353–365.
10. Slavič J and Boltežar M. Non-linearity and non-smoothness in multi-body dynamics: application to

- woodpecker toy. *Proc IMechE, Part C: J Mechanical Engineering Science* 2006; 220: 285–296.
11. Slavič J and Boltežar M. Measuring the dynamic forces to identify the friction of a graphite–copper contact for variable temperature and current. *Wear* 2006; 260: 1136–1144.
 12. Slavič J and Boltežar M. *Nonlinear and nonsmooth dynamics of discretely defined system of rigid bodies with unilateral contacts*. Doctoral Dissertation (no. 326), Faculty of Mechanical Engineering, University of Ljubljana, Ljubljana, 2005.
 13. Slavič J, Bryant MD and Boltežar M. A new approach to roughness-induced vibrations on a slider. *J Sound Vib* 2007; 306: 732–750.
 14. Ueno T, Kadono K and Morita N. Influence of surface roughness on contact voltage drop of electrical sliding contacts. In: *Proceedings of the fifty-third IEEE Holm conference on electrical contacts, 2007*, Pittsburgh, PA, 16–19 September 2007, pp.200–204. New York: IEEE.
 15. Ueno T, Morita N and Sawa K. Influence of surface roughness on voltage drop of sliding contacts under various gases environment. In: *Proceedings of the forty-ninth IEEE Holm conference on electrical contacts, 2003*, Washington, DC, 10 September 2003, pp.59–64. New York: IEEE.
 16. Ueno T and Morita N. Influence of surface roughness on contact voltage drop of sliding contacts. In: *Proceedings of the fifty-first IEEE Holm conference on electrical contacts, 2005*, Chicago, IL, 26–28 September 2005, pp.324–328. New York: IEEE.
 17. Zhongliang H, Zhenhua C, Jintong X, et al. Effect of PV factor on the wear of carbon brushes for micromotors. *Wear* 2008; 265: 336–340.
 18. Yasar I, Canakci A and Arslan F. The effect of brush spring pressure on the wear behaviour of copper–graphite brushes with electrical current. *Tribol Int* 2007; 40: 1381–1386.
 19. Barnawi E, Sawa K, Morita N, et al. The effect of various atmospheric temperature on the contact resistance of sliding contact on silver coating slip ring and silver graphite brush. In: *Proceedings of the 2011 IEEE 57th Holm conference on electrical contacts (Holm)*, Minneapolis, MN, 11–14 September 2011, pp.1–8. New York: IEEE.
 20. Wang YA, Li JX, Yan Y, et al. Effect of electrical current on tribological behavior of copper-impregnated metallized carbon against a Cu–Cr–Zr alloy. *Tribol Int* 2012; 50: 26–34.
 21. Wang Y, Zhang L, Wang T, et al. Effect of sliding velocity on the transition of wear mechanism in (Zr, Cu) 95Al5 bulk metallic glass. *Tribol Int* 2016; 101: 141–151.
 22. Fakih B and Dienwiebel M. The structure of tribolayers at the commutator and brush interface: a case study of failed and non-failed dc motors. *Tribol Int* 2015; 92: 21–28.
 23. Wang Y, Li J, Yan Y, et al. Effect of PV factor on sliding friction and wear of copper-impregnated metallized carbon. *Wear* 2012; 289: 119–123.
 24. Huda MD, Hashmi MSJ and El-Baradie MA. MMCs: materials, manufacturing and mechanical properties. *Key Eng Mater* 1995; 104–107: 37–64.
 25. Kogut L. Electrical performance of contaminated rough surfaces in contact. *J Appl Phys* 2005; 97: 103723.